Size Change of Dendrimers in Concentrated Solution

Andreas Topp,[†,§] Barry J. Bauer,[†] Ty J. Prosa,[†] Rolf Scherrenberg,[‡] and Eric J. Amis*[,†]

National Institute of Standards and Technology, Gaithersburg, Maryland 20899, and DSM Research, P.O. Box 18, 6160 MD, Geleen, The Netherlands

Received March 23, 1999; Revised Manuscript Received October 19, 1999

ABSTRACT: Solutions of the poly(propylene imine) dendrimers DAB-*dendr*-$(PA)_{32}$ and DAB-*dendr*-$(PA)_{64}$ in methanol are investigated with small angle neutron scattering over the range of dendrimer mass fraction $0.01 \leq x \leq 0.80$. The single particle scattering function, $P(q)$, is used to calculate the structure factor, $S(q)$, of the dendrimer solutions and to evaluate the radius of gyration of the dendrimers in dilute solution giving R_g^+(DAB-*dendr*-$(PA)_{32}$) = 12.4 ± 0.2 Å and R_g^+(DAB-*dendr*-$(PA)_{64}$) = (15.6 ± 0.2) Å. In each case the segment density in dilute solution is 0.35 ± 0.03 g cm^{-3}, leaving a large fraction of the dendrimer volume accessible to solvent. We define the "dilute solution regime" for dendrimers to extend to a concentration where the swollen dendrimer volume fraction first equals the value 0.64, which comes at a dendrimer weight fraction of $x = 0.25$. At this concentration, the spatial arrangement of the dendrimers can be described as a random close packing. For higher concentrations, the experimental scattering functions appear to be self-similar up to a mass fraction of $x \approx 0.60$. These observations are consistent with a model of concentrated dendrimer solutions which assumes that individual dendrimers collapse to maintain a volume fraction $\phi \approx 0.64$, which is the volume fraction of random close packing of hard spheres. Preliminary small X-ray scattering data give further evidence of the dendrimer collapse.

1. Introduction

Dendrimers are a new class of polymeric materials that can produce molecules with narrow molecular weight and physical size distributions. Dendrimers are very uniform when compared to other molecules in this class of polymers, such as hyperbranched and dendrigraft polymers. Hyperbranched polymers are commonly made by polymerizing trifunctional monomers in a single reaction step yielding materials with large polydispersity.[1] More recently, dendrigraft polymers have appeared, which are synthesized by grafting several linear polymers on a linear chain, and repeating the grafting step on the graft chains.[2] Although they can yield a more narrow distribution than hyperbranched polymers, these grafted polymers are not as highly branched as hyperbranched materials. Dendrimers achieve the objectives of a high degree of branching and a narrow molecular weight distribution by using specific chemical pathways to give molecules with relatively few topological defects[3,4] and are typically more uniform than linear polymers.

Dendrimers have the highest degree of perfection in a new class of highly branched polymers that has recently taken on an increased interest in macromolecular science. The precision of dendrimers is apparent when they are compared to other molecules in this class of polymers such as hyperbranched and dendrigraft polymers. Hyperbranched polymers are commonly made by polymerizing trifunctional monomers in a single reaction step, yielding materials with large polydispersity.[1] More recently, dendrigraft polymers have appeared, which are synthesized by grafting several linear polymers on a linear chain and repeating the grafting step on the graft chains.[2] Although they can yield a more narrow distribution, these grafted polymers are not as highly branched as hyperbranched materials. Dendrimers achieve the objectives of a high degree of branching and a narrow molecular weight distribution by using specific chemical pathways to give molecules with few topological defects.[3,4]

Since the first report of dendrimers by Tomalia et al.,[5] researchers in the field of dendrimer science have focused primarily on their synthesis and chemical modification. At present, a large variety of dendrimers, dendrimer chemistry, and sophisticated chemical modifications are known. Recently, work that is focused on characterization of dendrimers and dendritic materials has started to attract broader interest. Interestingly, this situation is also true for other highly branched polymers with only a few studies that show the variety of properties of hyperbranched polymers, dendrigraft materials, and dendrimers.[6−9] The results seem to indicate that the behavior of these molecules must be rationalized in a theoretical framework that includes the topological parameters of the polymer.

In this respect, it is interesting to compare the properties of star polymers that may also have a fairly perfect topology and spherical shape.[10] It is theoretically and experimentally well established that star polymers take an ordered spatial arrangement above the overlap concentration, and even form a crystalline order when the number of arms exceeds a certain threshold value.[11,12] No such phenomenon is seen for linear or lightly branched polymers.

We consider dendrimers to be an excellent reference material to study the effect of branching and topology on physical properties. In this report, we focus on the equilibrium dimensions of dendrimers in solution, covering the range of concentration from very dilute solutions to the bulk. In contrast to flexible linear chains, the phenomenology of concentrated dendrimer solutions is still a matter of speculation. Little is known about dendrimer−dendrimer interactions in concentrated solutions. For example, it is not clear whether the overlap

[†] National Institute of Standards and Technology.
[‡] DSM Research.
[§] Present address: Continental AG, Materials Research, Hannover, Germany.

10.1021/ma990433q CCC: $18.00
Published on Web 12/03/1999

concentration, c^*, as seen in solutions of neutral linear polymers, exists in dendrimer solutions. Thus, even a definition of "dilute" and "concentrated" regimes is lacking. This paper addresses some of these basic issues and defines language appropriate to classify dendrimer solutions.

Small-angle neutron scattering (SANS) experiments have been carried out with solutions of dendrimers in methanol over the range of mass fraction, x, between 0.01 and 0.80. Full and half generation poly(propylene imine) dendrimers, from generation 0.5 to generation 5, are currently available in quantity. Two generations of poly(propylene imine) dendrimers, DAB-*dendr*-$(PA)_{32}$ and DAB-*dendr*-$(PA)_{64}$, were used.[13−15] These dendrimers are terminated by primary amines (PA) and are grown from a tetrafunctional core of diaminobutane (DAB), resulting in 32 terminal PA units for DAB-*dendr*-$(PA)_{32}$, and 64 terminal PA units for DAB-*dendr*-$(PA)_{64}$.

2. Experimental Section

2.1. Materials. The poly(propylene imine) dendrimers were synthesized by DSM Research (Geleen, The Netherlands) according to reported procedures.[13−16] The theoretical molecular weights of the DAB-*dendr*-$(PA)_{32}$ and DAB-*dendr*-$(PA)_{64}$ are 3514 and 7168, respectively.[17] The glass transition temperatures are reported in the literature to be T_g(DAB-*dendr*-$(PA)_{32}$) = −87 °C and T_g(DAB-*dendr*-$(PA)_{64}$) = −84 °C. Both generations of the dendrimer are colorless, viscous liquids in bulk and are freely soluble in methanol.

2.2. Sample Preparation. The dendrimers DAB-*dendr*-$(PA)_{32}$ and DAB-*dendr*-$(PA)_{64}$ were used as received from DSM Research. The partially deuterated solvent CD_3OH (Aldrich Chem.) was used throughout the study. It is used instead of CD_3OD to prevent exchange of deuterium with the hydrogen of the terminal primary amines. All solutions were prepared gravimetrically to give mass fractions in the range $0.01 \le x \le 0.80$ for both generations (mass fractions studied: 0.01, 0.02, 0.03, 0.05, 0.10, 0.20, 0.30, 0.35, 0.40, 0.60, 0.80). A total of 12 h was allowed for dissolution before the solutions were transferred to quartz cells for the SANS experiments. The solutions of DAB-*dendr*-$(PA)_{64}$ appeared hazy by visual inspection. This impurity is likely to be the half-generation dendrimer that remained from the previous step.[18] After the solutions were centrifuged within the quartz cells at approximately 1200 times the force of gravity for 4 h, the solutions appeared clear and a trace of white residue was visible at the bottom of the cell and accounted for only a inconsequential fraction of the total solid. The residue was below the level of the neutron beam when these cells were used for the scattering experiments. Neat dendrimer DAB-*dendr*-$(PA)_{32}$ was also measured to yield a value for the incoherent scattering of the dendrimer. All SANS measurements were carried out at a temperature $T = 30.0$ °C, using a circulating bath with a known temperature range of less than ±0.1 °C.

2.3. Small Angle Neutron Scattering. The scattering experiments were performed at the 30m SANS facility (NG7; NIST/Exxon/U. Minn.) at the National Institute of Standards and Technology (Gaithersburg, MD).[19,20] The spectrometer was operated at a sample to detector distance of 110 cm, with a wavelength of $\lambda = 6$ Å, and a wavelength spread of $\Delta\lambda/\lambda = 0.15$. With this configuration, a wide range of the scattering vector, q, was covered ($0.05\ \text{Å}^{-1} \le q \le 0.55\ \text{Å}^{-1}$; with $q = (4\pi/\lambda)\sin(\theta/2)$, θ being the scattering angle). Two-dimensional intensity data were corrected for detector efficiency, background scattering, and the empty cell. A correction was also applied that corrects for the dependence of the path of a scattered neutron in the scattering sample on the scattering angle, and the depth at which the scattering event occurred.[21] The data were converted to absolute scattering intensities by use of an H_2O standard and the experimental transmission values. By circular averaging of two-dimensional data sets of the absolute intensities, the data were put in the final form of the absolute scattering intensity, I, as a function of the scattering vector q. The conversion of the data, as well as the corrections, was carried out on a μVAX 4000 computer with the software provided by the Cold Neutron Research Facility at NIST.[22] The incoherent scattering was subtracted from the data based on the appropriate fraction of scattering measured for pure solvent and for bulk dendrimer DAB-*dendr*-$(PA)_{32}$. Data analysis and error estimation are reported elsewhere.[19,20]

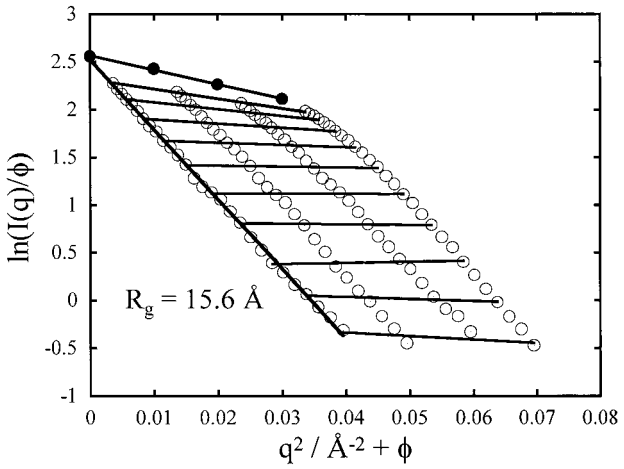

Figure 1. Natural log of reduced absolute scattering intensity, $\ln(I/\phi°)$, of solutions of DAB-*dendr*-$(PA)_{64}$ in CD_3OH as a function of the scattering vector q^2 for mass fractions in the range $0.01 \le x \le 0.03$ as indicated in the figure ($\phi°$, volume fraction of bulk dendrimer). Also shown are reduced intensity data that are extrapolated to $x \to 0$.

2.4. Small-Angle X-ray Experiments. SAXS experiments were carried out at the Advanced Polymers PRT beamline (X27C; SUNY Stony Brook/NIST/GE/Allied Signal/Montell) at the National Synchrotron Light Source, Brookhaven National Laboratory. A double-multilayer monochromator with an energy resolution ($\Delta E/E$) of 1% was used to obtain photons with a wavelength $\lambda = 1.304$ Å. A three pinhole collimation configuration defined a beam size of 0.1 mm, and a sample to detector distance of 1.05 m was used. This resulted in a measurable scattering range of $0.01\ \text{Å}^{-1} \le q \le 0.42\ \text{Å}^{-1}$. Beam monitors before and after the sample were used to normalize scattering intensities to the incident flux and to correct for transmission through the sample. Two-dimensional data sets were collected with Fuji Image Plates with a resolution of 0.2 mm ($\Delta q \approx 0.001\ \text{Å}^{-1}$). The SAXS solution cells had a path length of 4 mm and were equipped with thin mica windows of 6 μm thickness. Background intensities caused by scattering from the window of the detector vacuum chamber, solution cell, and beam stop were determined by separate measurements and subtracted from the sample data.

3. Results and Discussion

3.1. Low Concentration Solutions. SANS of dendrimer solutions of mass fractions $x = 0.01$, $x = 0.02$, and $x = 0.03$ was measured for both generations to characterize the average dimensions of the dendrimers. The measured scattering was used to calculate an experimental single particle scattering function, or experimental form factor, $P(q)_{exp}$, of the dendrimers. This form factor is used for analysis across the concentration regimes.

Data of absolute scattering intensity, $I(q)$, of DAB-*dendr*-$(PA)_{64}$ dendrimers are shown in Figure 1 as a function of the scattering vector q shown as a Guinier plot. To emphasize the effect of concentration on the scattering function, the intensity data are divided by the volume fraction of dendrimer, $\phi°$. The values of $\phi°$ are calculated for each mass fraction, x, according to the

following relationship:[23]

$$\phi^\circ = \frac{x/\rho^\circ}{(x/\rho^\circ) + ((1-x)/\rho_s)} \quad (1)$$

The solvent density, $\rho_s = 0.867$ g cm^{-3}, and the dendrimer bulk density, ρ° is 1.01 g cm^{-3}. Also shown in Figure 1 are the values of the reduced scattering intensity, $I(q, x\rightarrow 0)\phi^{\circ -1}$, that are extrapolated to a mass fraction $x\rightarrow 0$. This extrapolation was carried out by applying a nonweighted least-squares fit to the $I(q)\,\phi^{\circ -1}$ data in the range $0.01 \le x \le 0.03$, and results in the experimental form factor of the dendrimer, $P(q)_{exp}$ (the experimental standard deviation of the reduced scattering intensities, as well as the standard deviation of the values for $I(q, x\rightarrow 0)$, are covered by the size of the symbols of Figure 1).

The data at low-q in Figure 1 demonstrate that the reduced scattering intensity depends on the dendrimer mass fraction even at low concentrations. The values of the scattering intensity at low-q are depressed; the extent of this depression gradually increases with x. The observed deviation from the single particle scattering at low mass fraction of the dendrimers reflects the presence of a contribution from the interparticle structure factor, $S(q)$, to the scattering intensity $I(q)$. A more detailed discussion of $S(q)$, which represents the interparticle interactions and spatial correlations of the scattering molecules, will be deferred to the discussion of the high concentration regime. The uppermost line in Figure 1 is an extrapolation to $q = 0$. The downward slope of the line demonstrates that the second virial coefficient, A_2, is positive which is characteristic of a good solvent. The molecular weight of the dendrimers is too low to be reliably measured by SANS and cannot be used to estimate the chemical "perfection" of the dendrimers, but such a perfect structure will not be necessary to measure R_g changes.

The radius of gyration of the dendrimers in dilute solution, R_g^+, is calculated from the scattering intensities by fitting to the Guinier approximation[24] with the functional form

$$I(q) = a + b\,\exp\left\{-\frac{q^2 R_g^{\,2}}{3}\right\} \quad (2)$$

by a nonweighted nonlinear least-squares analysis. Since this analysis is based on the functional form of the form factor, the influence of structure factor contributions to the data will be apparent in the fitted values of R_g.

The values for the radii of gyration are found to be R_g^+(DAB-*dendr*-(PA)$_{32}$) = 12.4 ± 0.2 Å and R_g^+(DAB-*dendr*-(PA)$_{64}$) = 15.6 ± 0.2 Å, where the uncertainties of the values represent the standard deviation from the fits to the $I(q, x\rightarrow 0)$ data. These values are in reasonable agreement with the results of X-ray scattering in methanol solution[7] and a SANS study[25] of the dendrimers in D_2O, when we consider that those studies did not correct for effects of $S(q)$ on the calculated value of R_g^+. We note that R_g is relatively insensitive to solvent, an observation that will be expanded in a future paper.[26] A recently published paper has also considered interactions of dendrimers with ionic groups present.[27]

In Figure 2, the extrapolated SANS data ($I(q, x\rightarrow 0)\phi^{\circ -1}$) for DAB-*dendr*-(PA)$_{32}$ and DAB-*dendr*-(PA)$_{64}$, are shown

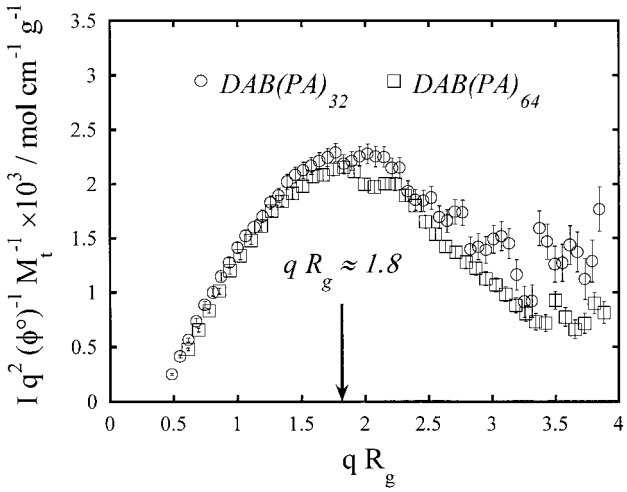

Figure 2. Kratky plot of the extrapolated SANS data ($I(q, x\rightarrow 0)/\phi^\circ$) for DAB-*dendr*-(PA)$_{32}$ and DAB-*dendr*-(PA)$_{64}$, normalized by the theoretical molecular weight, M_t. The experimental values of R_g^+ are used for the plot.

in a Kratky plot of the form $Iq^2R_g^+2\phi^{\circ -1}M^{-1}$ vs qR_g^+ using the experimental values for R_g^+, and reducing the data by the theoretical molecular weight M_t. A peak is observed at $qR_g^+ \approx 1.8$ for both generations, which is a common feature of the scattering function of spherical particles and particles with relatively high internal segment densities. Star scattering functions were first calculated by Benoit,[28] and a full review was given by Burchard.[29] For uniform spheres, the position of the peak is expected at $qR_g^+ \approx 1.7$. The characteristic peak in the Kratky plot is also observed for poly(amido amine) (PAMAM) dendrimers, as was shown by Bauer et al.[30,31] for generations G7 and G10. A detailed analysis of the internal structure and the polydispersity of is not necessary to the analysis of the high concentration interactions of dendrimers and is addressed in separate publications.[32]

In the present paper, the average segment density of the dendrimer is calculated from experimental values for R_g^+ under the assumption of uniform segment density. Under this condition, the radius of the dendrimer in dilute solution, R^+, can be calculated by using the relation $R^{+2} = {}^5/_3 R_g^{+2}$. The average density of the segments in the volume occupied by the dendrimer in solution, ρ^+, is given as

$$\rho^+ = \frac{M_t}{(4\pi/3)N_A R^{+3}} \quad (3)$$

with N_A being Avogadro's number. On the basis of the experimental value for R_g^+, the segment densities in dilute solution are ρ^+(DAB-*dendr*-(PA)$_{32}$) = 0.344 ± 0.026 g cm^{-3} and ρ^+(DAB-*dendr*-(PA)$_{64}$) = 0.345 ± 0.021 g cm^{-3} (the uncertainties are based on the standard deviation of the values of R_g^+).

The fractional volume in the dendrimer that is occupied by solvent can be calculated from the density as $C^+ = 1 - \rho^+/\rho^\circ$. This leads to $C^+ = 0.66 \pm 0.04$ for each generation and demonstrates the large volume inside a dendrimer accessible to solvent. Another way to express this observation is to calculate a hypothetical volume, or under the model of a uniform sphere, a hypothetical radius, R°, that the dendrimer would have at the bulk

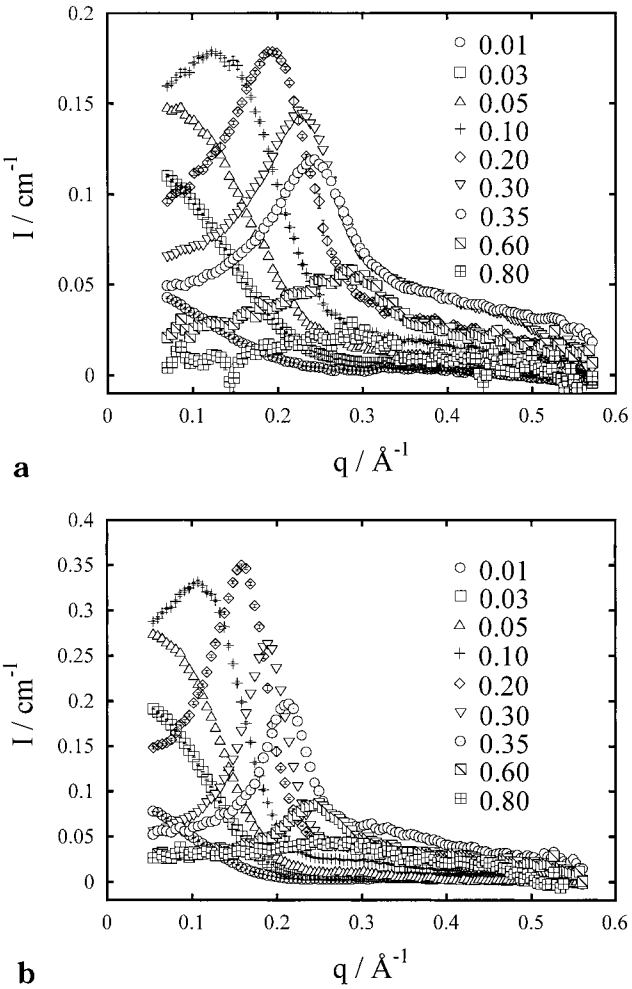

Figure 3. Absolute scattering intensity, I, from solutions of dendrimers in CD_3OH, as a function of the scattering vector q (the experimental standard deviation of the intensity, covered in most cases by the size of the symbols, is indicated by error bars) is shown for several values of the mass fraction of dendrimer, indicated in the figure: (a) dendrimer DAB-*dendr*-$(PA)_{32}$; (b) dendrimer DAB-*dendr*-$(PA)_{64}$.

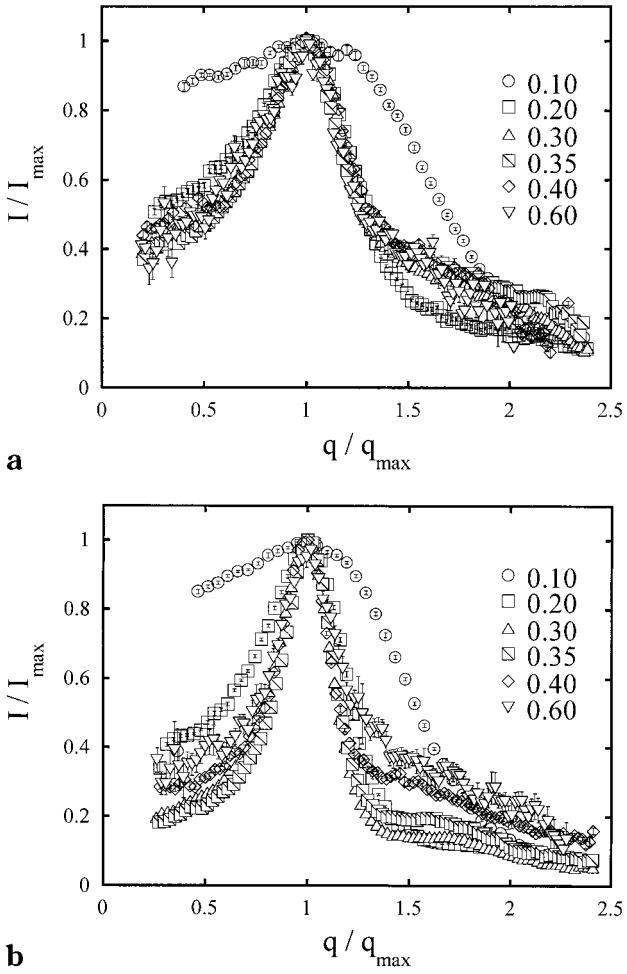

Figure 4. Normalized scattering intensity of the dendrimer solutions, I/I_{max}, plotted as a function of the normalized scattering vector q/q_{max} (values of the mass fraction x are indicated): (a) dendrimer DAB-*dendr*-$(PA)_{32}$; (b) dendrimer DAB-*dendr*-$(PA)_{64}$.

density. Using eq 3 and $\rho° = 1.01$ g cm^{-3} gives $R°$(DAB-*dendr*-$(PA)_{32}$) = 11.1 ± 0.19 Å and $R°$(DAB-*dendr*-$(PA)_{64}$) = 14.1 ± 0.26 Å. These values will be used in later discussions as estimates for limiting sizes of dendrimers that collapse with increasing concentrations to bulk density.

3.2. Concentrated Dendrimer Solution. Scattering Intensity. At very high dendrimer concentration, i.e., $x \geq 0.60$, the dominant amount of scattered intensity is incoherent due to the large fraction of hydrogen in the dendrimers. This leads to experimental uncertainty for the quantity of incoherent scattering that must be subtracted from the solution scattering intensity. This issue must be addressed carefully in the data analysis.

The scattering pattern exhibited by the solutions changes with increasing concentration of the dendrimers. In Figure 3, the absolute scattering intensity from the DAB-*dendr*-$(PA)_{32}$ and DAB-*dendr*-$(PA)_{64}$ solutions is shown as a function of q for the range of mass fraction $0.01 \leq x \leq 0.80$ (some data sets are omitted for clarity). The results for the different generations are qualitatively similar. A peak in the scattering intensity as function of q appears at a mass faction of $x = 0.10$. The intensity of the peak has its maximum value at $x \approx 0.20$ and decreases at higher mass fractions. Also, the position of the peak in the scattering function, q_{max}, is dependent on the dendrimer concentration, shifting to larger values of q with increasing mass fraction. This behavior is similar for both generations up to a mass fraction of $x = 0.80$.

The peak still appears in the scattering for a mass fraction as high as $x = 0.80$, but the relative intensity is very small. If the intensity data are normalized by the value of the maximum intensity I_{max} and the q values are normalized by that of the peak position, i.e., q_{max}, the resulting plots of I/I_{max} vs q/q_{max} are shown in Figure 4. The scattering functions for the dendrimer solutions are very similar in the range $0.20 \leq x \leq 0.60$; in particular the data in the range $0.30 \leq x \leq 0.60$ have a peak of the same shape and width. The relative intensity of the peak is also similar, but this value is somewhat uncertain for data of mass fraction $x = 0.60$, due to the uncertainty of the incoherent scattering as was mentioned previously. This suggests that solutions in the range $0.30 \leq x \leq 0.40$, and perhaps as high as $x = 0.60$, belong to the same concentration regime.

Structure Factor. The scattering patterns shown in Figures 3 and 4 result from a contribution by interparticle interactions that leads to spatial correlations for high number densities of the molecules. To analyze the scattering data in the high concentration range, we

extract the contributions arising from the interparticle correlations, i.e., the structure factor $S(q)$, from the experimentally observed small angle scattering. The function $S(q)$ is related to the pair distribution function by a Fourier transformation and contains the information of the spatial arrangement of the scattering units. For a dispersion of identical particles, the scattering intensity can be expressed as

$$I(q) = \phi f^2 P(q) S(q) \tag{4}$$

where ϕ is the volume fraction of the particles and f is the scattering amplitude of the isolated scattering particle at zero angle.[24] By applying this relationship to dendrimer solutions, we make use of the so-called "decoupling approximation"; i.e., we assume that the intraparticle scattering can be separated from intermolecular interaction effects. Equation 4, in combination with the decoupling approximation, is commonly applied for the treatment of scattering data, and is used extensively in the field of dispersed colloids and polymers.[10] By rearrangement of eq 4, it is obvious that the structure factor can be calculated from the scattering data by division of $I(q)$ by ϕ and the particle form factor, $P(q)$. It is necessary to assume that $P(q)$ does not change with concentration.

In section 3.1, we have shown that the scattering intensities from the dilute solutions in the range $0.01 \le x \le 0.03$ can be extrapolated to $I(q, x \rightarrow 0)$ to give an experimental form factor. The extrapolated data are fitted in a semi-phenomenological approach to an equation of the functional form of eq 2 to give an apparent form factor $P(q)_{app}$ for DAB-*dendr*-$(PA)_{32}$ and DAB-*dendr*-$(PA)_{64}$. Following the notation of eq 4, we use

$$P(q)_{app} \equiv I(q, x \rightarrow 0) \cong f^2 P(q) \tag{5}$$

to reduce the scatter in the data for the calculation. Using the volume fraction of dendrimer from eq 1, $\phi°$, we compute an apparent structure factor, $S(q, x)_{app}$, according to the expression

$$S(q, x)_{app} = \frac{I(q, x)}{\phi° P(q)_{app}} \tag{6}$$

This procedure is only exact if the form factor of the particle, which is determined in the limit $x \rightarrow 0$, remains unchanged at the concentration of the experiment. This assumption is expected to be valid for dilute and moderately concentrated dendrimer solutions, but may become less justified at higher dendrimer concentrations. For clarity, we omit the notation of the mass fraction, x, and write $S(q)_{app}$ instead of $S(q, x)_{app}$. The calculations of the structure factors are given in Appendix 1.

On the basis of the radius R^+ of dendrimers in dilute solution, one can calculate the concentration at which these molecules would fill the volume of the solution. The structure factors of the dendrimer solutions (see Figures 7 and 8 in the Appendix) show a strong excluded volume effect, causing a locally ordered but noncrystalline arrangement in concentrated solution. This requires that the dendrimers as a whole do not interpenetrate freely, indicating at least partial dendrimer-dendrimer exclusion. This finding can be rationalized by either of the two models. One approach is to picture the dendrimers to consist of an inner volume, or core, which is purely noninterpenetrable and is surrounded by a shell of a certain thickness that can be occupied by segments of different dendrimers. In this model, the dendrimers could keep the same size in concentrated solution as they have in dilute solution. This can be referred to as partial interpenetrating dendrimers. The second model pictures a dendrimer that exclude all segments of different dendrimers from the volume it occupies. Here, the dendrimers are completely noninterpenetrable, and therefore they have to shrink at high concentrations due to packing arguments, leading to a concentration-dependent radius of the dendrimers. This can be referred to as noninterpenetrating dendrimers. This case is analogous to the model of partial interpenetrating dendrimers in the limit of an infinitely thin interpenetrable shell.

The structure factors calculated in this section cannot conclude if interpenetration of the segments of different dendrimers is completely prohibited or not. However, other experiments can be used to build the case. By direct visualization using cryo−electron micrographs, dendrimer solutions show no indication of dendrimer−dendrimer interpenetration.[33] Also, we will show small-angle X-ray data indicating that dendrimers are individual entities, even at high concentration, thus supporting the model of noninterpenetrating dendrimers. This model is assumed in the following discussion of the experimental structure factors of the dendrimers solutions.

Intermolecular Spacing. The values of q_{max} are related to a mean value of the distance between the centers of the dendrimers, Λ, as

$$\Lambda = 1.22 \frac{2\pi}{q_{max}} \tag{7}$$

which, strictly speaking, is derived for the case of uniform spherical particles on a face-centered cubic lattice.[24] In the preceding section, it was shown that the dendrimers under study do not form a crystalline arrangement in solution. Nonetheless, this relation is employed commonly to discuss the interparticle spacing in uniform, densely packed but noncrystalline systems. For example, this relation gives useful values for the center-to-center distance of densely packed particles such as star polymers.[34,35] In the case of dendrimers, the uniformity of the molecular shape and size makes the use of eq 7 reasonable. The notation Λ_{app} is used to indicate the inherent assumptions. Figure 5 shows $\Lambda_{app}/2$ plotted as a function of the mass fraction of dendrimer, x, for both generations.

We note that the shape of the experimental structure factors extracted from scattering data, and the positions of the peaks do not strongly depend on the values of R_g used to estimate the form factor. We tested this by using model form factors calculated with R_g values ranging from the dilute solution value down to the hypothetical limiting size that the dendrimer would occupy if it collapsed to a sphere with bulk dendrimer density. The measured values of Λ_{app} do not change significantly.

It is interesting to calculate the mass fraction x^*_{RCP} of dendrimers necessary to achieve random close packing of their dilute solution radii, R^+. This concentration is shown in Figure 5 by the dashed vertical lines. Also shown, with horizontal dashed lines, are the values of $\Lambda_{app}/2$ that are equal to the dilute solution dendrimer radii and the hypothetical limiting size, $R°$, that the

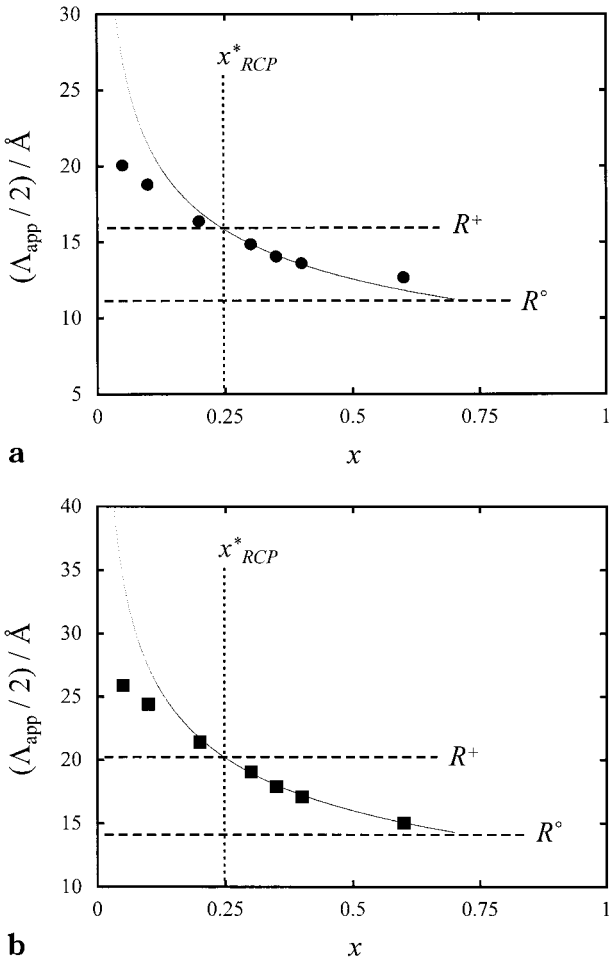

Figure 5. Plot of the apparent mean distance between the centers of DAB-*dendr*-$(PA)_x$ dendrimers, Λ_{app}, vs the mass fraction dendrimer, x. Also shown are dotted and broken lines that indicate reference values as described in the text. Key: (a) dendrimer DAB-*dendr*-$(PA)_{32}$; (b) dendrimer DAB-*dendr*-$(PA)_{64}$.

dendrimers would occupy if they collapsed to a density equal to the density of bulk dendrimers. The curves in Figure 5 represent a calculation of the variation of $\Lambda_{app}/2$ for repulsive particles exhibiting random close packing. The observation that the dendrimer spacing, $\Lambda_{app}/2$, crosses the intersection of R^+ and x^*_{RCP} and decreases to approach the value of the dendrimer radius at bulk density, suggests that they resemble repulsive spheres dispersed in random close packing.

The fact that the values $\Lambda_{app}/2$ are smaller than the radius of the dendrimer in dilute solution for mass fractions x greater than 0.24 means that either interpenetration occurs or the dendrimers collapse, leading to $R_{app} < R^+$. This result holds over the range of concentration from 0.24 to 0.6 (see Figure 5), which is the range in which the normalized scattering intensities are self-similar, as shown in Figure 4. In the limit of high mass fraction, the values of R_{app} approach the value $R°$ that is the hypothetical size for individual dendrimers having a density equal to the neat dendrimer bulk density.

Under the assumption that dendrimers collapse to this bulk density we can calculate the dendrimer solution concentration where the volume fraction of dendrimers, ϕ^+, would equal the random close packed volume fraction, $x^*_{RCP} = 0.64$. Using these values of $\rho°$, and $R°$, for the solvent CD_3OH, the RCP mass fraction

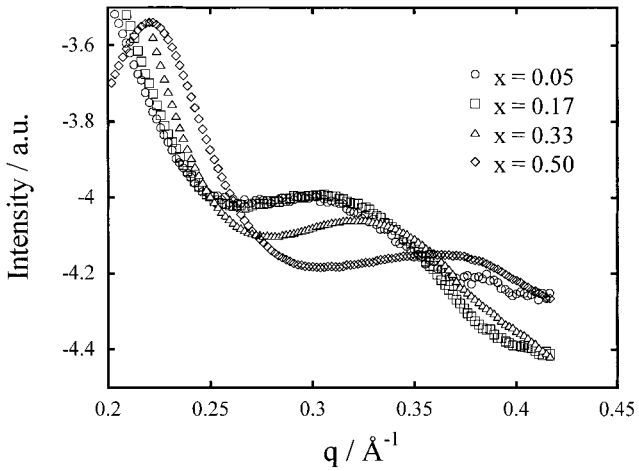

Figure 6. Semilogarithmic plot of the small-angle X-ray scattering intensity, I, of solutions of DAB-*dendr*-$(PA)_{64}$ in CH_3OH, normalized by the mass fraction, as a function of the scattering vector q (mass fractions, x, are indicated).

is 0.67. For higher concentrations, we can speculate that if the dendrimers still do not show significant interpenetration, they must shrink more or undergo a change in shape in order for concentrations to be greater than 0.64. A tempting view is the limit of a "soap bubble like" picture, where the dendrimer-dendrimer interface becomes more and more continuous with increasing number density, leading to smaller cavities that can be preferentially occupied by solvent molecules. At some point, the cavities vanish, and the solvent is solely incorporated in the dendrimer, using its remaining solvent capacity. This leads, in the limit of bulk dendrimer, to a continuous interface between the dendrimers.

Intramolecular Form Factor. It has been shown for poly(amido amine) dendrimers that the uniform size and shape of dendrimers in solution give rise to higher order features in the scattering function which are well described by the theoretical scattering function of a uniformly dense sphere.[7,30−31] The q values of the maxima and minima of these higher order peaks are directly related to the size of the sphere.[24] Higher order features remain also at high concentrations, as long as the molecules are still spherical and uniform. These features can be used to calculate the radius of the molecules in the high-q range if the structure factor has reached a constant value, $S(q) = 1$, and does not affect the scattering function. This has been demonstrated with latex-dispersions, for which the higher order peaks of a crystallized dispersion are identical to the features of dilute dispersions.[36] Hence, in the range of concentration where the dendrimers collapse, on the basis of the model of random close packing, the higher order features of the dendrimer scattering can persist and the change in size should result in a shift of the peak positions of the higher order features to higher values.

Due to the large amount of incoherent scattering, these higher order features cannot be resolved by SANS. Instead, small-angle X-ray scattering (SAXS) can be used to overcome this limitation in a study of DAB-*dendr*-$(PA)_{64}$ in CH_3OH in the range of concentration $0.05 \le x \le 0.50$.[37] In the absence of the large incoherent background, and with the high flux provided by a synchrotron beam, we resolve the higher order features for the dendrimer solutions. In Figure 6, the high-q range of the experimental X-ray scattering intensity is

shown, normalized by the mass fraction of the dendrimers in a semilogarithmic plot. A higher order feature around $q = 0.03$ Å^{-1} can be clearly identified for the low concentrations. We point out that the occurrence of the higher order peak at $x = 0.05$ demonstrates that the maximum is not due to oscillations in interparticle the structure factor. It is due to the single particle form factor and demonstrates that the size and shape of the dendrimers are spherical with low polydispersity. This higher order feature remains for concentrations up to $x = 0.50$. For the concentration $x = 0.17$, the position of the maximum remains virtually unchanged from the dilute solution limit, indicating that the dimensions of the dendrimers are also the same. For the concentrations $x = 0.33$ and $x = 0.50$ the location of the maximum shifts to higher values of q, demonstrating that the size of the dendrimers changes in high concentration dendrimer solutions. Equally important, the existence of higher order features in high concentrated dendrimer solutions indicates that the molecules are still individual entities, and remain nominally spherical under these conditions. This suggests that no significant dendrimer−dendrimer interpenetration occurs, and it is in accord with the ideal model of noninterpenetrating collapsing dendrimers in high concentration solutions.

A recent scanning force microscopy study of arborescent polystyrenes by Sheiko et al. has shown that ordered monolayer films of these cascade-branched polymers can be achieved that consist of individual molecules.[38] In case of a high branching density, the molecules deform to an elipsoidal shape during the monolayer formation, but recover to a spherical geometry when annealed above their glass transition temperature. The radius of the cascade-branched polymers corresponds well to the radius of bulk density particles. In the case of poly(amido amine) dendrimers, TEM micrographs also show no indication of interpenetration.[33] A comparison of various branched structures in dilute solution by small angle scattering techniques has revealed that repulsion is generally observed and it gains strength with increasing branching density and uniformity of the molecules.[6,7] A comparison of these observations with the results of the present report suggests that a high branching density leads to a strong tendency of the molecules to avoid interpenetration.

In the case of star polymers of high functionality, osmotic repulsion is strong enough to force the molecules to form ordered arrangements in the vicinity of the overlap concentration.[10] However, the absence of interpenetration also for systems that lack any solvent, as observed in the monolayer films of annealed arborescent graft polystyrene, may indicate that the driving force to avoid intermixing of highly branched molecules is different from the case of star polymers. Sheiko et al. argue that the conservation of entropic elasticity could be the reason for the suppression of interpenetration.[38] Presently, this view is consistent with our studies. However, a theoretical framework is lacking and more experimental work is needed to further elucidate the phenomenology of highly branched macromolecules.

4. Conclusions

We can suggest an idealized view of poly(propylene imine) dendrimers DAB-*dendr*-$(PA)_{32}$ and DAB-*dendr*-$(PA)_{64}$ in solution that is consistent with a model of noninterpenetrating collapsing dendrimers. We can see varied behavior at different concentrations and describe the two ranges. The notations are for dissolved compact molecules such as dendrimers and should not be confused with similar terms used for other dispersions such as colloids.

Dilute Solution, $x \leq x^*_{RCP}$. We can define the "dilute solution regime" for dendrimers to be the range where the dendrimer volume fraction ϕ^+ is smaller than the threshold value $\phi_{RCP} = 0.64$, i.e., the dendrimer mass fraction x is smaller than x^*_{RCP}. Dendrimers in dilute solution behave as a dispersion of soft spheres; these are uniform and have spherical shape. The dimensions can be expressed by the radius of gyration R^+_g, or, under the valid assumption of uniform segment density, by the outer radius of the spherical dendrimer in dilute solution, R^+. The structure factor for the scattering from the dendrimer solution appears at very low concentration. No significant interpenetration occurs between the segments of different dendrimers. For $\phi^+ < 0.64$, the size of the dendrimer is not strongly affected by the concentration of dendrimers in solution.

Concentrated Solution, $x \geq x^*_{RCP}$. At concentrations larger than x^*_{RCP}, the size of the molecules decreases as their number density increases. The dendrimers collapse in an amount that yields a constant volume fraction of $\phi \approx 0.64$. We refer to this picture as "random close packing of collapsing dendrimers." We do not have evidence that this RCP behavior continues to higher mass fractions than would be required to cause the RCP dendrimers to collapse to bulk density. At those concentrations we speculate that the dendrimers would deform from their spherical shape and fill the voids between the spheres much like "grapes" shrinking and deforming to become "raisins".

Although we have shown, on the basis of preliminary results from small-angle X-ray scattering, that the dendrimer collapse can be followed by the first higher order peak of the dendrimers, a more extensive SAXS study is needed to study the collapse of dendrimers at high concentration. In addition, SANS experiments that use the contrast match technique with solutions of deuterated dendrimers mixed with nondeuterated dendrimers should allow direct observation of the collapse of dendrimers.

Acknowledgment. The authors gratefully acknowledge valuable discussions with Dr. Jack Douglas. A. Topp gratefully acknowledges the financial support by the Deutsche Forschungsgemeinschaft. This material is based upon work supported in part by the U.S. Army Research Office under Contract No. 35109-CH.

Appendix

The apparent structure factors for the dendrimers DAB-*dendr*-$(PA)_{32}$ and DAB-*dendr*-$(PA)_{64}$, calculated from the neutron scattering, are shown in Figure 7 for the range of mass fraction $0.05 \leq x \leq 0.30$ (the data of $S(q)_{app}$ are offset by a constant for clarity; the error bars indicate the value of the experimental uncertainty of $S(q)_{app}$, as calculated from the standard deviation of $I(q)$ and $P(q)_{app}$ by using the Gauss law of error propagation). At high-q values, the apparent structure factors of dendrimer solutions with mass fractions $x \leq 0.30$ approach the value 1 within the experimental uncertainty, with the exception of the data of $x = 0.30$ for DAB-*dendr*-$(PA)_{64}$. Reaching the theoretical value of a structure factor in the high-q limit confirms the validity of the analysis with its inherent assumptions. For the

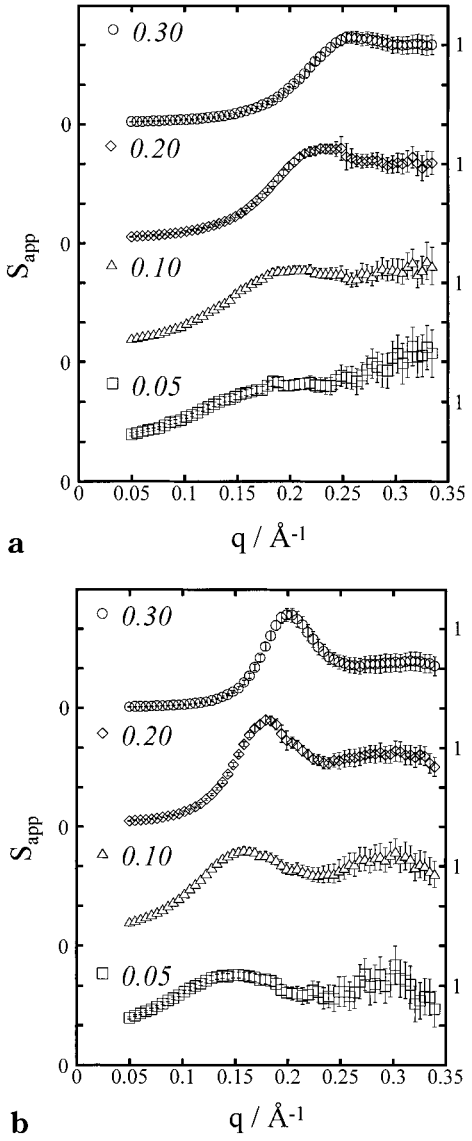

Figure 7. Apparent structure factor, S_{app}, for dendrimer solutions of different mass fractions $x \leq 0.30$, plotted vs the scattering vector q and offset by a constant for clarity; the values of the mass fraction are indicated. Key: (a) dendrimer DAB-*dendr*-$(PA)_{32}$; (b) dendrimer DAB-*dendr*-$(PA)_{64}$.

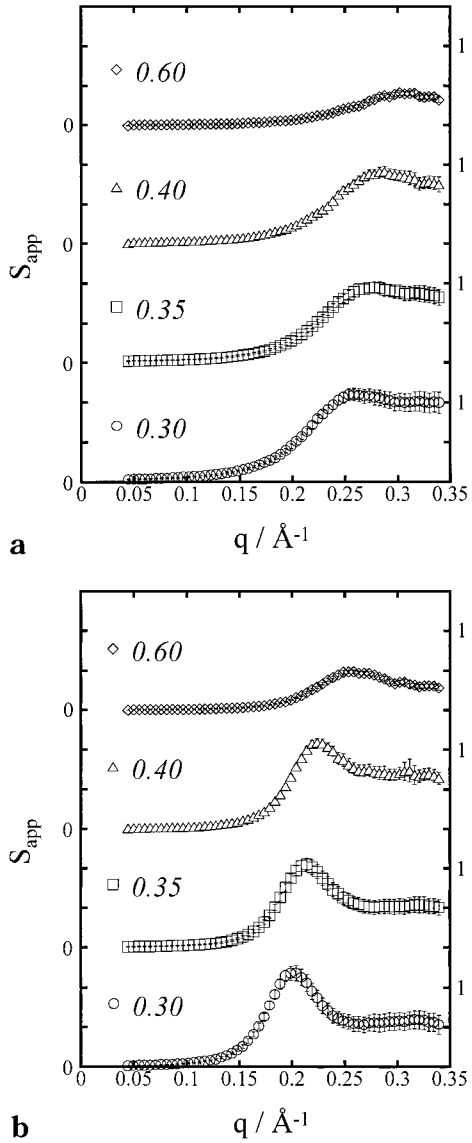

Figure 8. Apparent structure factor of dendrimer solutions of $x \geq 0.30$, plotted as in Figure 7. Key: (a) dendrimer DAB-*dendr*-$(PA)_{32}$; (b) dendrimer DAB-*dendr*-$(PA)_{64}$.

low-q limit, we find that the value of $S(q \rightarrow 0)_{app}$ is a decreasing function of x, and approaches zero at mass fractions $x \geq 0.20$.

For the mass fraction x > 0.30, the calculated structure factors no longer reach the value of 1 in the high-q limit, as shown in Figure 8. This is expected to occur at high mass fraction, because the decoupling approximation becomes poorer. Also, the use of the particle form factor $P(q)_{app}$ is no longer exact, since the size of the dendrimer is a function of concentration. The other features of $S(q)_{app}$, i.e., being zero in the low-q limit and having a maximum, remain unchanged for the solutions with large dendrimer content. The peak position is insensitive to the $P(q)_{app}$ that is used.

Currently, no theoretical approach or simulation exists that considers highly concentrated dendrimer solutions, i.e., dendrimer−dendrimer interactions or $S(q)$ of dendrimer solutions. Therefore, further analysis will be based on a comparison with results from hard sphere systems and solutions of star polymers. We emphasize that the dendrimers themselves are not considered to be hard spheres. From the amount of flexibility, reflected by the amount of swelling in solution as described in section 3.1, the dendrimers are better described as soft spheres with an unknown amount of fuzzyness at the outside. However, we expect hard spheres and star polymers to be suitable reference systems for dendrimer solutions, since the dendrimers are distinct spherical molecules with a negligible polydispersity.[6,7]

For an ensemble of monodisperse particles, the value of the structure factor in the zero-q limit, $S(q \rightarrow 0)$, is directly proportional to the isothermal compressibility and reflects the nature of the effective pair potential.[39] This correspondence is experimentally well established by various scattering techniques, for example with dispersions of spheres and star polymer solutions.[21,40] The presence of adhesive interactions between the scattering particles (for example "sticky spheres") leads to a pronounced upturn of $S(q)$ at low-q values, whereas in the case of a hard-sphere potential or repulsive interactions, the values of $S(q)$ approach zero in the low-q limit.[41,42] The low-q limit of the apparent structure factors of dendrimer solutions, shown in parts a and b

of Figure 7, indicates that the pair potential of the poly(propylene imine) dendrimers DAB-*dendr*-$(PA)_{32}$ and DAB-*dendr*-$(PA)_{64}$ in methanol is repulsive.

The structure factor is the Fourier transformation of the pair distribution function, thus it contains the information about the spatial arrangement of the scattering particles. In Figure 7b and Figure 8b it is shown that $S(q)_{app}$ exhibits a maximum for the dendrimer DAB-*dendr*-$(PA)_{64}$. This maximum is comparably weak for the dendrimer DAB-*dendr*-$(PA)_{32}$, but still detectable (see Figure 7a and Figure 8a). Also, the value of the momentum transfer where the maximum in $S(q)$ is found, q_{max}, shifts to larger values of q with increasing dendrimer content of the solution. The presence of a peak indicates that the dendrimers have spatial first neighbor correlations. From the height of the peak it follows that no long-range order is formed, since the threshold value for crystalline materials, $S(q_{max}) \approx 2.7$, is never reached. Instead, the maximum value of the peak is $S(q_{max}) \approx 1.2$ for the generation 4 dendrimer, and $S(q_{max}) \approx 1.4$ for the generation 5 dendrimer. These values are comparable to those from hard-sphere dispersions of homogeneous or Gaussian scatterers and to those from star polymers at the overlap concentration that have a functionality f below the threshold f_c where crystalline ordering occurs.[7,43−44]

References and Notes

(1) Fréchet, J. M. J.; Hawker, C. J.; Gitsov, I.; Leon, J. W. *J. Macromol. Sci., Pure Appl. Chem.* **1996**, *A33*, 1399.
(2) Tomalia, D. A.; Hedstrand, D. M.; Ferritto, M. S. *Macromolecules* **1991**, *24*, 1435.
(3) Tomalia, D. A.; Naylor, A. M.; Goddard, W. A. *Angew. Chem., Int. Ed. Engl.* **1990**, *29*, 138.
(4) Ardoin, N.; Astruc, D. *Bull. Soc. Chim. Fr.* **1995**, *132*, 875.
(5) Tomalia, D. A.; Baker, H.; Dewald, J.; Hall, M.; Kallos, G.; Martin, S.; Roeck, J.; Ryder, J.; Smith, P. *Polym. J.* **1985**, *17*, 117.
(6) Bauer, B.; Topp, A.; Prosa, T. J.; Amis, E. J.; Yin, R.; Qin, D.; Tomalia, D. A. *ACS PMSE Proc.* **1997**, *77*, 87.
(7) Prosa, T. J.; Bauer, B. J.; Amis, E. J.; Tomalia, D. A.; Scherrenberg, R. J. *J. Polym. Sci., Polym. Phys. Ed.* **1997**, *35*, 2913.
(8) Hawker, C. J.; Malmström, E. E.; Frank, C. W.; Kampf, J. P.; Mio, C.; Prausnitz, J. *ACS PMSE Proc.* **1997**, *77*, 61.
(9) Tomalia, D. A.; Dvornic, P. R.; Uppuluri, S.; Swanson, D. R.; Balogh, L. *ACS PMSE Proc.* **1997**, *77*, 95.
(10) Grest, G. S.; Fetters, L. J.; Huang, J. S.; Richter, D. *Adv. Chem. Phys.* **1996**, *154*, 67.
(11) Roovers, J. *Macromolecules* **1994**, *27*, 5359.
(12) Richter, D.; Jucknischke, O.; Willner, L.; Fetters, L. J.; Lin, M.; Huang, J. S.; Roovers, J.; Toporovski, C.; Zhou, L. L. *J. Phys. IV, Suppl. JP I* **1993**, *3*, 3.
(13) de Brabander-van den Berg, E. M. M.; Meijer, E. W. *Angew. Chem., Int. Ed. Engl.* **1993**, *32*, 1308.
(14) de Brabander-van den Berg, E. M. M.; Nijenhuis, A.; Mure, M.; Keulen, J.; Reintjens, R.; Vandenbooren, F.; Bosman, B.; de Raat, R.; Frijns, T.; v.d. Wal, S.; Castelijns, M.; Put, J.; Meijer, E. W. *Macromol. Symp.* **1994**, *77*, 51.
(15) de Brabander-van den Berg, E. M. M.; Brackman, J.; Mure-Mak, M.; de Man, H.; Hogeweg, M.; Keulen, J.; Scherrenberg, R.; Coussens, B.; Mengerink, Y.; van der Wal, S. *Macromol. Symp.* **1996**, *102*, 9.
(16) Certain commercial materials and equipment are identified in this paper in order to specify adequately the experimental procedure. In no case does such identification imply recommendation by the National Institute of Standards and Technology nor does it imply that the material or equipment identified is necessarily the best available for this purpose.
(17) According to ISO 31−8, the term "Molecular Weight" has been replaced by "relative Molecular Mass," symbol M_r. Thus, if this nomenclature and notation were to be followed in this publication, one would write $M_{r,n}$ instead of the historically conventional M_n for the number-average molecular weight, with similar changes for M_w, M_z, and M_v, and it would be called the "number Average Relative Molecular Mass." The conventional notation, rather that the ISO notation, has been employed for this publication.
(18) Private communications.
(19) Prask, H. J.; Rowe, J. M.; Rush, J. J.; Schröder, I. G. J. *Res. Natl. Inst. Stand. Technol.* **1993**, *98*, 1.
(20) Hammouda, B.; Krueger, S.; Glinka, C. *J. Res. Natl. Inst. Stand. Technol.* **1993**, *98*, 31.
(21) Vineyard, G. H. *Phys. Rev.* **1954**, *96*, 93.
(22) *SANS Data Reduction and Imaging Software*; Cold Neutron Research Facility, NIST: Gaithersburg, MD, 1996.
(23) Values for the densities as given in the product specification by the manufacturer; no attempt was undertaken to verify the values.
(24) Guinier, A.; Fournet, G. *Small Angle Scattering of X-rays*; Wiley: New York, 1955.
(25) Scherrenberg, R.; Coussens, B.; van Vliet, P.; Edouard, G.; Brackman, J.; de Brabander, *Macromolecules* **1998**, *31*, 456.
(26) Topp, A.; Bauer, B. J.; Tomalia, D. A.; Amis, E. J. Submitted for publication in *Macromolecules*.
(27) Ramzi, A.; Scherrenberg, R.; Brackman, J.; Joosten, J.; Mortensen, K. *Macromolecules* **1998**, *31*, 1621.
(28) Benoit, H. *J. Polym. Sci.* **1953**, *11*, 507.
(29) Burchard, W. *Adv. Polym. Sci.* **1983**, *48*, 1.
(30) Bauer, B.; Briber, R. M.; Hammouda, B.; Tomalia, D. A. *ACS PMSE Proc.* **1992**, *67*, 428.
(31) Bauer, B.; Hammouda, B.; Briber, R. M.; Tomalia, D. A. *ACS PMSE Proc.* **1994**, *69*, 342.
(32) Amis, E. J.; Topp, A.; Bauer, B. J.; Tomalia, D. A. *ACS PMSE Proc.* **1997**, *77*, 183.
(33) Jackson, C. L.; Chany, H. D.; Booy, F. P.; Drake, B. J.; Tomalia, D. A.; Bauer, B. J.; Amis, E. J. *Macromolecules* **1998**, *31*, 6259.
(34) Huber, K.; Bantle, S.; Burchard, W.; Fetters, L. *Macromolecules* **1986**, *19*, 1404.
(35) Willner, L.; Jucknischke, O.; Richter, D.; Farago, B.; Fetters, L. J.; Huang, J. S. *Europhys. Lett.* **1992**, *19*, 297.
(36) Megens, M.; van Kats, C. M.; Bösecke, P.; Vos, W. L. To be published in *J. Appl. Cryst.*
(37) Prosa, T. J.; Bauer, B. J.; Topp, A.; Amis, E. J.; Scherrenberg, R. *ACS PMSE Proc.* **1998**, *79*, 307.
(38) Sheiko, S. S.; Gaithier, M.; Möller, M. *Macromolecules* **1997**, *30*, 2343.
(39) Hansen, J. P.; McDonald, I. R. *Theory of Simple Liquids*; Academic Press: London, 1979.
(40) Roovers, J.; Toporowski, P. M.; Douglas, J. *Macromolecules* **1995**, *28*, 7065.
(41) Robertus, C.; Philipse, W. H.; Joosten, J. G. H.; Levine, Y. K *J. Chem. Phys.* **1989**, *90*, 4482.
(42) Woutersen, A. T. J. M.; May, R. P.; de Kruif, C. G. *J. Rheol.* **1993**, *37*, 71.
(43) van Beurten, P.; Vrij, A. *J. Chem. Phys.* **1981**, *74*, 2744.
(44) Witten, T. A.; Pincus, P. A.; Cates, M. E. *Europhys. Lett.* **1986**, *2*, 137.

MA990433Q